Chemical Vapor Deposition of Boron Nitride Nanosheets on Metallic Substrates via Decaborane/Ammonia Reactions

Shahana Chatterjee,[†] Zhengtang Luo,[*,‡] Muharrem Acerce,[‡] Douglas M. Yates,[§] A. T. Charlie Johnson,[‡] and Larry G. Sneddon[*,†]

[†]Department of Chemistry, University of Pennsylvania, Philadelphia, Pennsylvania 19104-6323, United States

[‡]Department of Physics and Astronomy, University of Pennsylvania, Philadelphia, Pennsylvania 19104-6396, United States

[§]Laboratory for Research on the Structure of Matter, University of Pennsylvania, Philadelphia, Pennsylvania 19104-6202, United States

S *Supporting Information*

Both graphene, an atomically single-layer sheet of sp^2-bonded graphitic carbon, and multilayer carbon nanosheets (CNS) have been of intense research interest because of their remarkable electronic, mechanical, and optical properties.[1] Hexagonal boron nitride (h-BN) is the structural analog of graphite, where alternating boron and nitrogen atoms replace carbon atoms in the sp^2 lattice structure. While retaining the mechanical properties and high thermal conductivity of graphite, the elemental substitution in h-BN results in a number of property changes, including a large band gap (>5 eV) and enhanced oxidation resistance.[2] These differences make nanostructured BN uniquely attractive for applications in nanoelectronics, optoelectronics and nanocomposites.[3]

BN nanosheets (BNNS) were first isolated by Pacile et al, who employed micromechanical cleavage using adhesive tape to peel off BN layers from h-BN powder.[4a] Others achieved solution exfoliation of BN layers from h-BN flakes using sonication in the presence of polar solvents and/or reagents.[4b−d] BNNS have also been obtained by laser ablating a h-BN target.[5] The first synthetic routes to BNNS involved the reactions of boron oxides with either urea[6a] or melamine[6b] and boric acid with melamine.[6c] More recently, chemical vapor deposition (CVD) methods, employing the thermal decomposition of the amineboranes, ammonia-borane[7a,b] and borazine,[7c] on metal or graphene substrates and the plasma-induced reactions of BF_3 in a H_2/N_2 atmosphere[7d] have been shown to produce BNNS. We report here a convenient method, involving the reaction of the commercially available polyborane decaborane with ammonia, that provides a simple CVD route for the efficient formation of BNNS on either polycrystalline Ni or Cu foils.

Decaborane ($B_{10}H_{14}$), the most widely available neutral polyborane, has a number of properties[8] that have made it an attractive reagent for CVD generation of boron containing materials: (1) it is easy to handle since it is an air and moisture stable crystalline solid (unlike borazine)[9] that does not decompose up to ~300 °C under inert conditions and (2) its easily regulated vapor pressure over the RT-90 °C range[8] allows it to be readily sublimed without decomposition (unlike ammonia-borane)[10] into the gas phase so that it can be transported into the reaction zone of a CVD furnace by an inert carrier gas. Previously, CVD methods have been used to generate micrometer-scale BN films from decaborane on nonmetallic substrates, including amorphous BN films on silicon and sapphire wafers by thermal CVD of decaborane/ammonia mixtures[11] and crystalline BN films on GaAs or Si substrates by plasma enhanced CVD of decaborane in ammonia or nitrogen.[12]

Previous work has demonstrated that BN monolayers could be grown on single-crystal metals[13−15] by the thermal decomposition of borazine[13a,14] or B-trichloroborazine[13b] under ultra high vacuum conditions. The excellent lattice match of h-BN with the 111 faces of Ni or Cu facilitated BN growth on these metals. Following these reports, polycrystalline Ni and Cu were shown to be catalytic substrates for the growth of BNNS from the amineborane precursors.[7a−c] We have now found that the thermal CVD of decaborane/ammonia mixtures on these polycrystalline metal substrates also generate crystalline BNNS.

The metal foils were first annealed in the CVD system shown in Figure S1 in the Supporting Information to 1000 °C under a combined flow of nitrogen and hydrogen. At 1000 °C, the hydrogen flow was stopped and decaborane vapors, produced by heating the vessel containing solid decaborane with a heating tape at ~70 °C, were carried into the furnace using a nitrogen carrier gas that was combined with a mixed ammonia and nitrogen carrier stream as they entered the furnace. After growth for 10 min, the BNNS films were annealed under a mixed ammonia and nitrogen flow for 10 min. The films were then cooled to RT under a mixed ammonia and nitrogen stream.

For subsequent analyses, the as-grown BNNS films were first spin-coated with poly(methylmethacrylate) (PMMA) and then the metal substrates were etched away by treatment with ~3N HCl (Ni)[16a] or a ~2.5% $FeCl_3$ solution (Cu).[16b] For analysis by optical microscopy and AFM, the resulting BNNS/PMMA films were washed with deionized water and then transferred to SiO_2/ Si wafers where the PMMA layer was removed by first washing with acetone followed by annealing under hydrogen to remove residual carbon. For TEM analyses, the BNNS/PMMA films were transferred to copper grids coated with holey carbon films, with the PMMA then removed by acetone washing.
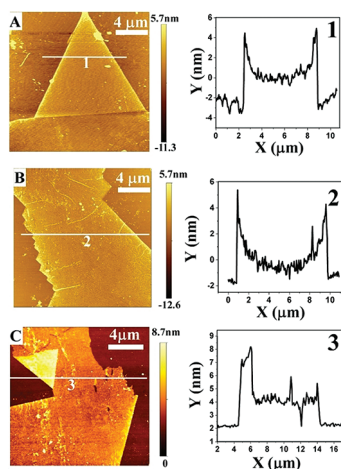
Figure 1. AFM images and height profiles of BNNS grown on Ni-foil exhibiting an average thickness of ∼2 nm and angular edges: (A) a BNNS with a triangular shape; (B) a BNNS with zigzag and straight edges; (C) a BNNS with a large folded-over section.

The optical and atomic force microscopy (AFM) images showed that the BNNS grown on both Ni (optical image, Figure S2A in the Supporting Information; AFM images Figure 1, left) and Cu (optical image, Figure S2B in the Supporting Information; AFM images, Figure S3 in the Supporting Information) have large areas that are tens to hundreds of micrometers in length. The AFM analyses in the tapping mode in Figure 1 (right) indicate that the films grown on Ni are ∼2 nm thick on average, corresponding to only a few layers of BN graphene (a 1−3 layered graphene film on SiO_2/Si wafer has been found to be ∼1.0−1.6 nm).[1a] As can be seen in Figures 1A and 1B, the BNNS were generally found to be thicker (4−6 nm) at the sheet edges as a result of either edge wrinkling or folding. Similar types of features have previously been observed in CNS.[17] Although the BNNS were grown on Ni and Cu under the same deposition conditions, AFM analysis of the films on Cu showed that they were generally thicker, ranging from 2 to 15 nm (Figure S3 in the Supporting Information). As can be seen in Figure 1C for Ni and Figure S3B in the Supporting Information for Cu, in several cases, a fold over of a large section[1a] of a sheet was observed to give a region that was of increased thickness. Many of the BNNS grown on Ni exhibited well-defined angular edges, with near regular angles of 30, 60, or 90°. Similar regular angular features have been observed in the hexagonal domains of graphene grown via methane CVD on copper foils under low precursor pressures.[18] Likewise, the BN monolayers reported on Ni (111) initially nucleate to form BN domains with perfectly angular edges.[13b,19] Thus, a fine-tuning of the decaborane/ammonia pressure and growth conditions may likewise result in the controlled growth of regular polygonal BNNS structures on metallic substrates.

Transmission electron microscopy (TEM) at 200 kV was used to estimate the number of layers and analyze the fine structure of the BNNS. The low magnification images again confirmed the formation of BNNS on Ni with large micrometer-scale areas with some crumpling and folding (Figure 2A) similar to those found in CNS.[20] At higher magnification, the individual layers of the folded edges were resolved (Figure 2B−E). As in CNS, the folded edge of a bilayer BNNS is observed as two dark lines in its TEM image.[20] Hence, for both CNS and BNNS, the number of
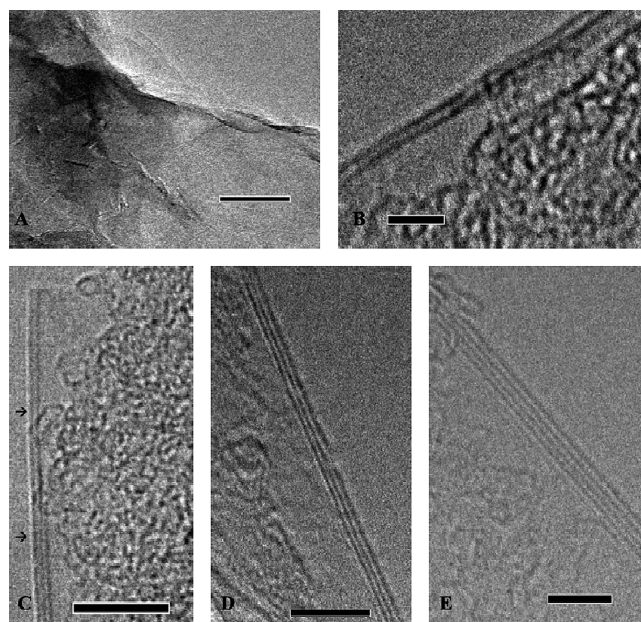

Figure 2. TEM images of BNNS: (A) a low-magnification image of the BNNS showing the formation of micrometer scale sheets; (B−E) high-magnification images of a two-, three-, and four-layered BNNS, C has BNNS with two layers in the top half and three layers in the lower half. Scale bars: A, 100 nm; B, 2 nm; and C−E, 5 nm.

layers may be simply determined by counting the number of dark lines in their TEM images. Most of the BNNS deposited on Ni were two- or three-layered (Figure 2B−D); however, in agreement with the AFM analyses, some regions were thicker (Figure 2E), containing up to six layers. Consistent with bulk h-BN, the separation between each sheet was ∼0.34 nm.[2] The high-resolution TEM image in Figure 3 of a BNNS surface showed a crystalline lattice structure characteristic of h-BN.[2]

As shown in Figure S5 in the Supporting Information, qualitative analyses of the BNNS by electron energy loss spectroscopy (EELS) confirmed the presence of B and N. The BNNS spectra are similar to the EELS spectra of bulk h-BN, with the sharp and well-defined peaks at ∼189 meV and ∼399 meV corresponding to the K shell excitations of B and N, respectively.[21]

The Raman spectra shown in Figure S6 in the Supporting Information of the BNNS also confirmed the formation of h-BN.[7,22] showing the characteristic E_{2g} vibration at ∼1366 cm^{-1} with an intensity that increased as the film thickness was increased, Figures S6A (∼6 nm) and S6B (∼10 nm) in the Supporting Information. These peaks were broader than that obtained from an ∼2 nm BNNS obtained by exfoliation from h-BN flakes (Figure S6C in the Supporting Information), consistent with less-ordered structures for the CVD grown BNNS. The electron diffraction images in Figure 3 (inset) of the BNNS grown on Ni exhibited (100) and (110) ring patterns characteristic of polycrystalline BN.[7d]

In conclusion, the syntheses of BNNS by the CVD method reported herein from the convenient, commercially available decaborane precursor now provides a simple way of generating BNNS on either polycrystalline Ni or Cu foils. Further improvements in this decaborane/ammonia process will likely require a more detailed understanding of the BNNS growth mechanism(s) on these substrates. Decaborane is known to react at high temperatures with many metals to form metal borides[23] and this coupled with the fact that nickel boride has been shown to catalyze[24] the
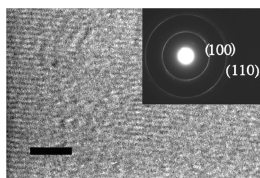
Figure 3. High-magnification TEM image of the BNNS surface showing a crystalline h-BN lattice structure, scale bar = 2 nm. Inset: Electron diffraction pattern obtained from BNNS grown on Ni.

formation of BN nanotubes, suggests that metal boride formation could be involved in at least initially seeding BNNS growth. However, it may well prove that, like in graphene,[25] the growth mechanisms may be quite different on the Ni and Cu substrates with factors such as relative boron solubility and ease of metal boride formation each playing roles.

ASSOCIATED CONTENT

Ⓢ **Supporting Information.** Descriptions of experimental procedures; Figure S1, schematic diagram of the CVD system; Figure S2, optical images of BNNS grown on (A) Ni (B) Cu foils; Figure S3, AFM images and height profiles of BNNS grown on Cu; Figure S4, TEM images of BNNS grown on Cu; Figure S5, EELS of BNNS grown on Ni; Figure S6, Raman spectra of BNNS grown on Ni and exfoliated BNNS. This material is available free of charge via the Internet at http://pubs.acs.org.

AUTHOR INFORMATION

Corresponding Author
*E-mail: ztom.luo@gmail.com (Z.L.); lsneddon@sas.upenn.edu (L.G.S.).

ACKNOWLEDGMENT

REFERENCES

(1) (a) Novoselov, K. S.; Geim, A. K.; Morozov, S. V.; Jiang, D.; Zhang, Y.; Dubonos, S. V.; Grigorieva, I. V.; Firsov, A. A. *Science* **2004**, *306*, 666–669. (b) Geim, A. K. *Science* **2009**, *324*, 1530–1534. (c) Allen, M. J.; Tung, V. C.; Kaner, R. B. *Chem. Rev.* **2010**, *110*, 132–145.

(2) (a) Meller, A. *Gmelin Handbook of Inorganic and Organometallic Chemistry*; Springer-Verlag: Berlin, 1991; 4th supp., Vol. 3a, pp 1−152. (b) Paine, R. T.; Narula, C. K. *Chem. Rev.* **1990**, *90*, 73–91.

(3) (a) Watanabe, K.; Taniguchi, T.; Kanda, H. *Nat. Mater.* **2004**, *3*, 404–409. (b) Zhi, C.; Bando, Y.; Tang, C.; Kuwahara, H.; Golberg, D. *Adv. Mater.* **2009**, *21*, 2889–2893. (c) Yu, J.; Qin, L.; Hao, Y.; Kuang, S.; Bai, X.; Chong, Y.-M.; Zhang, W.; Wang, E. *ACS Nano* **2010**, *4*, 414–422. (d) Golberg, D.; Bando, Y.; Huang, Y.; Terao, T.; Mitone, M.; Tang, C.; Zhi, C. *ACS Nano* **2010**, *4*, 2979–2993. (e) Golberg, D.; Bando, Y.; Huang, Y.; Xu, Z.; Wei, X.; Bourgeois, L.; Wang, M.-S.; Zeng, H.; Lin, J.; Zhi, C. *Isr. J. Chem.* **2010**, *50*, 405–416.

(4) (a) Pacile, D.; Meyer, J. C.; Girit, C. O.; Zettl, A. *Appl. Phys. Lett.* **2008**, *92*, 133107/1–133107/3. (b) Han, W.-Q.; Wu, L.; Zhu, Y.; Watanabe, K.; Taniguchi, T. *Appl. Phys. Lett.* **2008**, *93*, 223103/1–223103/3. (c) Lin, Y.; Williams, T. V.; Xu, T.-B.; Cao, W.; Elsayed-Ali, H. E.; Connell, J. W. *J. Phys. Chem. C* **2011**, *115*, 2679–2685. (d) Lin, Y.; Williams, T. V; Connell, J. W. *J. Phys. Chem. Lett.* **2010**, *1*, 277–283.

(5) Zhang, H. X.; Sajjad, M.; Feng, P. X. *Mater. Res. Soc. Symp. Proc.* **2010**, *1259*, S14−10/1–6.

(6) (a) Nag, A.; Raidongia, K.; Hembram, K. P. S. S.; Datta, R.; Waghmare, U. V.; Rao, C. N. R. *ACS Nano* **2010**, *4*, 1539–1544. (b) Gao, R.; Yin, L.; Wang, C.; Qi, Y.; Lun, N.; Zhang, L.; Liu, Y.-X.; Kang, L.; Wang, X. *J. Phys. Chem. C* **2009**, *113*, 15160–15165. (c) Zhu, Y.; Bando, Y.; Yin, L.; Golberg, D. *Nano Lett.* **2006**, *6*, 2982–6.

(7) (a) Ci, L.; Song, L.; Jin, C.; Jariwala, D.; Wu, D.; Li, Y.; Srivastava, A.; Wang, Z. F.; Storr, K.; Balicas, L.; Liu, F.; Ajayan, P. M. *Nat. Mater.* **2010**, *9*, 430–435. (b) Song, L.; Ci, L.; Lu, H.; Sorokin, P. B.; Jin, C.; Ni, J.; Kvashnin, A. G.; Kvashnin, D. G.; Lou, J.; Yakobson, B. I.; Ajayan, P. M. *Nano Lett.* **2010**, *10*, 3209–3215. (c) Shi, Y.; Hamsen, C.; Jia, X.; Kim, K. K.; Reina, A.; Hofmann, M.; Hsu, A. L.; Zhang, K.; Li, H.; Juang, Z.-Y.; Dresselhaus, M. S.; Li, L.-J.; Kong, J. *Nano Lett.* **2010**, *10*, 4134–4139. (d) Qin, L.; Yu, J.; Li, M.; Liu, F.; Bai, X. *Nanotechnology* **2011**, *22*, 215602/1–215602/7.

(8) (a) *Gmelin Handbuch der Anorganischen Chemie, Boron-Hydrogen Compounds*; Springer-Verlag: Berlin, 1979; new supp. series; Vol. 54, p 122−209. (b) Perel, A. S.; Loizides, W. K.; Reynolds, W. E. *Rev. Sci. Instrum.* **2002**, *73*, 877–879.

(9) *Gmelin Handbuch der Anorganishen Chemie, Borazine and Its Derivatives*; Springer-Verlag: Berlin, 1978; new supp. series, Vol. 51, pp 25−35.

(10) (a) Stephens, F. H.; Pons, V.; Baker, R. T. *Dalton Trans.* **2007**, 2613–2626. (b) Wolf, G.; Baumann, J.; Baitalow, F.; Hofmann, F. P. *Thermochim. Acta* **2000**, *343*, 19–25.

(11) Nakamura, K. *J. Electrochem. Soc.* **1985**, *132*, 1757–1762.

(12) (a) Kim, Y. G.; Dowben, P. A.; Spencer, J. T.; Ramseyer, G. O. *J. Vac. Sci. Technology A* **1989**, *7*, 2796–9. (b) Zhang, Z.; Kim, Y. G.; Dowben, P. A.; Spencer, J. T. *Mater. Res. Soc. Symp. Proc.* **1989**, *131*, 407–412.

(13) (a) Nagashima, A.; Tejima, N.; Gamou, Y.; Kawai, T.; Oshima, C. *Phys. Rev. Lett.* **1995**, *75*, 3918–3921. (b) Auwarter, W.; Suter, H. U.; Sachdev, H.; Greber, T. *Chem. Mater.* **2004**, *16*, 343–345.

(14) Preobrajenski, A. B.; Vinogradov, A. S.; Martensson, N. *Surf. Sci.* **2005**, *582*, 21–30.

(15) Paffett, M. T.; Simonson, R. J.; Papin, P.; Paine, R. T. *Surf. Sci.* **1990**, *232*, 286–296.

(16) (a) Reina, A.; Jia, X.; Ho, J.; Nezich, D.; Son, H.; Bulovic, V.; Dresselhaus, M. S.; Kong, J. *Nano Lett.* **2009**, *9*, 30–35. (b) Luo, Z.; Lu, Y.; Singer, D. W.; Berck, M. E.; Somers, L. A.; Goldsmith, B. R.; Johnson, A. T. C. *Chem. Mater.* **2011**, *23*, 1441–1447.

(17) Chae, S. J.; Gunes, F.; Kim, K. K.; Kim, E. S.; Han, G. H.; Kim, S. M.; Shin, H.-J.; Yoon, S- M.; Choi, J.-Y.; Park, M. H.; Yang, C. W.; Pribat, D.; Lee, Y. H. *Adv. Mater.* **2009**, *21*, 2328–2333.

(18) (a) Robertson, A. W.; Warner, J. H. *Nano Lett.* **2011**, *11*, 1182–1189. (b) Yu, Q.; Jauregui, L. A.; Wu, W.; Colby, R.; Tian, J.; Su, Z.; Cao, H.; Liu, Z.; Pandey, D.; Wei, D.; Chung, T. F.; Peng, P.; Guisinger, N. P.; Stach, E. A.; Bao, J.; Pei, S.-S.; Chen, Y. P. *Nat. Mater.* **2011**, *10*, 443–449.

(19) Auwarter, W.; Muntwiler, M.; Osterwalder, J.; Greber, T. *Surf. Sci.* **2003**, *545*, L735–L740.

(20) Meyer, J. C.; Geim, A. K.; Katsnelson, M. I.; Novoselov, K. S.; Booth, T. J.; Roth, S. *Nature* **2007**, *446*, 60–63.

(21) (a) Ahn, C. C.; Krivanek, O. L. *EELS Atlas* 1983, Gatan Inc., PA, USA. (b) Loiseau, A.; Willaime, F.; Demoncy, N.; Hug, G.; Pascard, H. *Phys. Rev. Lett.* **1996**, *76*, 4737–4740. (c) Arenal, R.; Stephan, O.; Loiseau, A.; Colliex, C. *Microsc. Microanal.* **2007**, *13* (Suppl. 2), 1240(CD)–1241CD.

(22) Geick, R.; Perry, C. H. *Phys. Rev.* **1966**, *146*, 543–547.

(23) (a) Su, K.; Sneddon, L. G. *Chem. Mater.* **1993**, *5*, 1659–1668. (b) Kher, S. S.; Spencer, J. T. *Chem. Mater.* **1992**, *4*, 538–544.

(24) (a) Lourie, O. R.; Jones, C. R.; Bartlett, B. M.; Gibbons, P. C.; Ruoff, R. S.; Buhro, W. E. *Chem. Mater.* **2000**, *12*, 1808–1810. (b) Tang, C.; Bando, Y.; Sato, T. *Chem. Phys. Lett.* **2002**, *362*, 185–189.

(25) Li, X.; Cai, W.; Colombo, L.; Ruoff, R. S. *Nano Lett.* **2009**, *9*, 4268–4272.

4416

dx.doi.org/10.1021/cm201955v | *Chem. Mater.* 2011, 23, 4414–4416